A SIMULATION OF A FEEDFORWARD NEURAL NETWORK FOR THE AUTOMATIC CONTROL OF A FOUR-WHEEL-STEERING PASSENGER CAR

Sohair F. Rezeka

Department of Mechanical Engineering, Faculty of Engineering,
Alexandria University, Alexandria, Egypt.

ABSTRACT

An automatic control system using a feedforward neural network is proposed for four-wheel-steering passenger cars to mimic the behavior of human driver. The control system consists of two identical two-layer-feedforward networks and a feedback of the car heading deviation. One neural network acts as an emulator, and the second represents a feedforward controller. The synaptic weights of the networks are adjusted according to the generalized adaline weight adaptation algorithm. The duration of the general learning was 500 s, and no measurements were acquired. Computer simulation was carried out to evaluate the performance of the proposed system in tasks involving lane keeping on a curving roadway at different speeds, gusting side wind, and an obstacle-avoidance maneuver. The results showed that the system displayed good driving performance, and was capable of reproducing the steering performance of human driver. The system realized rapid, comfortable, and stable responses in the different tasks.

Keywords: Neural network, Steering, Auto pilot.

INTRODUCTION

Four-wheel-steering (FWS) systems for automobiles have been actively studied as one of the latest automotive technologies. Properly designed systems can improve the maneuverability of vehicles at low speed and cruising stability at high speed. A simple speed-dependent ratio between rear and front wheels was used in an open-loop controller to achieve zero steady-state, side-slip angle during directional maneuvers [1]. This controller is simple but it may not perform well during transient motion. On the contrary, closed-loop controllers are robust and improve directional stability because they modify the driver steering command to the vehicle's front and rear steering wheels according to measured vehicle conditions. Whithead [2] examined a linear feedback combination of yaw rate and front-wheel steer angle to command rear-wheel steer angle. Lee [3] investigated the LQR control law in both stability and command augmentation systems to improve the response to disturbances at highway speeds on straight roads. Karnopp et al. [4]

illustrated the potential improvements as well as limitations inherent when the rear wheels, the front wheels, or both were steered by a feedback control scheme. Xia et al. [5] used a nonlinear bicycle model of an automobile, and linear control law with speed-based gains to examine the response of the vehicle to combined steering and braking inputs. Ackermann et al. [6] derived a robust decoupling control law by feedback of the yaw rate to both the front and rear wheel steering.

The implementation of model dynamics of driver steering enhanced the development of advanced vehicle steering. Lee [7] addressed the control-law design of a preview steering autopilot for an FWS vehicle to perform automatic lane tracking. The steering autopilot design was formulated as an optimal, discrete-time preview path tracking problem under the "perfect measurement" assumption. Modjtahedzadeh et al. [8] presented a theoretical control model of the behavior of driver steering. The model contains both preview and compensatory

elements. With these classical models, the control provides robustness over a small range of uncertainty. In addition, the control modes cannot cope with sudden changes of a payload due to gusting wind and changes in cruising velocity. Since the model of driver steering should be based on physiological and morphological information, neural networks may be considered in this application.

A neural network (NN) is a system of interconnected elements modeled after the human brain. With neural networks, the problem of control can be considered as a pattern-recognition problem. The pattern to be recognized is "change signal" that maps into "action signal" for specified system performance. The intelligent controller should recognize and isolate patterns of change in real time and "learn" from experience to recognize the change more quickly, even with incomplete data. The properties of pattern recognition and mapping with ever-improving self-organization and decision making are some of the potential advantages when using artificial neural networks for design and implementation of intelligent controllers [9]. Shiotsuka et al. [10] have recently used NN to control an FWS car. They applied two kinds of active-control systems. In the first system, NN was used to adapt the feedforward and backward gains of the controller. This system was simple but unreliable. In the second system back-propagation trained NN was used to generate the rear steer angle only, while the front steer angle was the driver input. Although the latter was reliable, the design was complex, acquiring measured data, and the learning time was long.

The objective of this paper is to implement neural network-based control to mimic the behavior of human driver by generating the steer angles of both front and rear wheels. The performance of the controller is evaluated in tasks ranging from lane keeping on a curving roadway to an obstacle avoidance. The effects of side wind and braking maneuver on the system response are also examined.

STEERING DYNAMICS MODEL

The essential features of car steering dynamics in a horizontal plane are described by the "bicycle model" shown in Figure (1). In this model it is

assumed that: 1) the vehicle is symmetrical about a longitudinal plane through the center of gravity, 2) relatively small yaw rate and lateral velocities are experienced by the vehicle in high-speed cruise, 3) the relatively small aligning torques are neglected, and 4) there is no pitch, roll, or heave motion and no longitudinal velocity perturbations. It should be noted that friction at wheels is not included in the model since frictionless wheels represent the worst condition with respect to steerability. On the other hand, the friction force at the wheel will not be greatly affected either by the load or by the road condition because such a state-of-the-art car is equipped with an active suspension and an antilock braking system. The active suspension reduces the fluctuations in wheel-to-road contact force, while the antilock brake minimizes the slip for the four wheels. Therefore, the friction force can be considered as disturbance load which can be adapted during the learning mode.
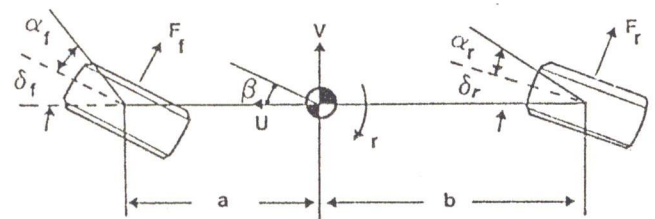

Figure 1. Bicycle model for car steering.

Since the forward speed, U, is kept constant, the resulting model has two degrees of freedom represented by the lateral velocity v, and the yaw rate r. The equations of motion are derived as (Appendix A):

$$I_{zz}\dot{r} + \frac{(a^2 C_{\alpha f} + b^2 C_{\alpha r})}{U}r + \frac{(a C_{\alpha f} - b C_{\alpha r})}{U}v = a\,C_{\alpha f}\delta_f - b\,C_{\alpha r}\delta_r - L\,W \quad (1)$$

$$M_s\dot{v} + (M_s U + \frac{(a C_{\alpha f} - b C_{\alpha r})}{U})r + \frac{C_{\alpha f} + C_{\alpha r}}{U}v = C_{\alpha f}\delta_f + C_{\alpha r}\delta_r - W \quad (2)$$

where a and b denote the distances between the vehicle c.g. and both front and rear axles, respectively. M_s nd I_{zz} are the mass and the yaw

moment of inertia of the vehicle, respectively. $C_{\alpha f}$ and $C_{\alpha r}$ represent the front and rear cornering stiffness of each tire, respectively. δ_f and δ_r are the front and rear steer angles. W is the wind load and L is the location of the center of pressure.

Figure (2) shows the lane-tracking steering geometry. S is a curvilinear distance variable measured along the centerline of the roadway. The rate of change of the heading of the local tangent to roadway with respect to S defines the roadway curvature ρ_r. Considering $\Delta\psi$ and Δy as the heading and lateral offset of the vehicle c.g. from the centerline of the roadway, then the following relations hold for small v/U and $\Delta\psi$

$$\Delta\psi \approx r - U \rho_r \qquad (3)$$

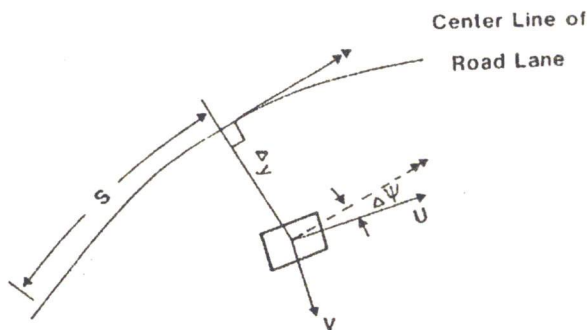$$\Delta\dot{y} \approx U \Delta\psi + v \qquad (4)$$

Figure 2.. Lane tracking geometry.

NEURAL-NETWORK MODEL

Artificial neural networks (ANN) can be classified according to their feedback link connection structure into: 1) recurrent (global feedback connection), e.g., Hopfield NN, 2) locally recurrent (local feedback connection), e.g., cellular NN, and 3) nonrecurrent (no feedback connection),e.g., perceptions. A special type of nonrecurrent ANN is the feedforward neural network (FNN). It consists of layers of neurons with synaptic weighted links connecting the outputs of neurons in one layer to the input of neurons in the next layer. Psaltis et al. [11] used an FNN-based feedforward controller within a general plant control system. They proposed general and specialized learning architectures that used the error back

propagation method to adjust the FNN link weights. Kawato et al. [12] used a feedback error learning architecture to teach the inverse dynamic model of a voluntary movement to an FNN. Their control architecture has the following advantages: First, the desired output of the inverse dynamics model is not required. Second, learning and control are done on-line. Third, error back propagation through the plant is not required. Nguyen et al. [13] showed that FNN can learn on its own to control a nonlinear dynamical system. They used two FNN's as an emulator and a controller. Chen [14] used back-propagation trained FNN within a self-tuning control system to control single-input single-output feedback linearizable system. Excellent tracking results were obtained for a nonlinear system but the training time was excessive. Kuschewski et al. [15] discussed methods for identification and control of a dynamical system by adaline, two-layer, and three-layer FNN using generalized adaline weight adaptation algorithms. Good results were obtained and learning time was short. None of the previous papers addressed FWS steering control except Shiotsuka et al. [10] who ,as stated earlier , applied the error back-propagation method.

In this work, a two-layer FNN and the generalized adaline weight adaptation algorithms [15] are used to control both the front and rear steer angles. The weight adaptation algorithm is presented in the next section.

Two-Layer FNN Weight Adaptation Algorithm

A block diagram of the two-layer FNN is showed in Figure (3). At the time increment k, $x \varepsilon R^n$ is the input signal vector which is assumed to be constant during the time increment. $W1_k \varepsilon R^{n1*n}$ is the first synaptic weight matrix. $\Gamma \varepsilon R^{n1}$ is an odd activation operator, $z_k \varepsilon R^{n1}$ is the input vector to Γ and $y1_k \varepsilon R^{n1}$ is the output vector of Γ. $W2_k \varepsilon R^{n2*n1}$ is the second synaptic weight matrix. y_k and y_d are the output and the desired output vector. e_k is the output error vector. n1, and n2 are the number of neurons in the first and second layer, respectively. The synaptic weight adaptation algorithm is given by:

$$W1_{k+1} = W1_k + \Delta W1_k \qquad (5)$$

where

$$\Delta W1_k = \frac{-2z_k\,\theta_1^T(x)}{\theta_1^T(x)x} \quad \text{if} \quad \theta_1^T(x)x \neq 0$$

$$= \quad 0 \quad \text{if} \quad \theta_1^T(x)x = 0$$

$$W2_{k+1} = W2_k + \Delta W2_k$$

where

$$\Delta W2_k = -2W2_k - \frac{Ae_k\theta_2^T(y1_k)}{\theta_2^T(y1_k)y1_k} \quad \text{if} \quad q \neq 0$$

$$= \quad 0 \quad \text{if} \quad q = 0$$

$$q = \theta_2^T(y1_k)\,y1_k$$

and

$$e_{k+1} = (I_{n2} - A)\,e_k$$
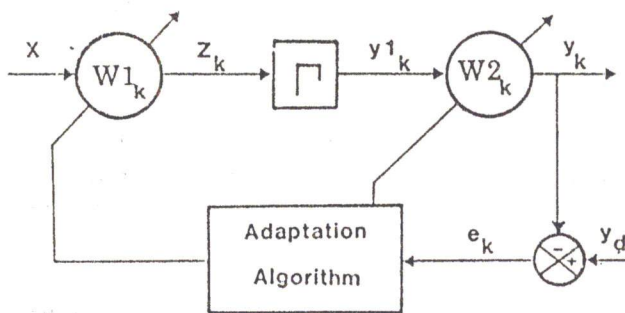
Figure 3. Block diagram of a two-layer FNN.

θ_1 and θ_2 are odd operators, I is the identity matrix, and $A \in R^{n2*n2}$ is the error reduction matrix. To obtain the asymptotic error converging to zero, A must be chosen such that the eigne values of $(I_{n2}-A)$ are placed in the left-hand side of the complex plane.

FNN-Based Controller

An ideal sampler (IS) of sampling period T and zero-order hold (ZOH) are connected to the FNN for input signal sampling. The three connected elements represent the FNN module (FNNM). The block diagram of the control circuit is shown in Figure (4). Two identical FNNM in conjunction with a feedback of the heading deviation are used. The master FNNM is employed as an emulator. The slave FNNM represents the neural feedforward controller. It acts as the inverse of the plant, producing from the desired yaw rate the steer angles which drive the vehicle. The input to The FNN is the desired yaw rate with n=3 and sampling period of 0.05 seconds. The number of neurons in the first layer is 6 and in that in the second layer is 2. The neurons activation operator is chosen as $\Gamma(x)=x$. The operators in the weight adaptation algorithm θ_1, and θ_2 are chosen as sgn(x) where

$$sgn(x) = \quad +1 \quad \text{if} \quad x > 0$$

$$= \quad -1 \quad \text{if} \quad x < 0$$

For accurate training , A is selected as

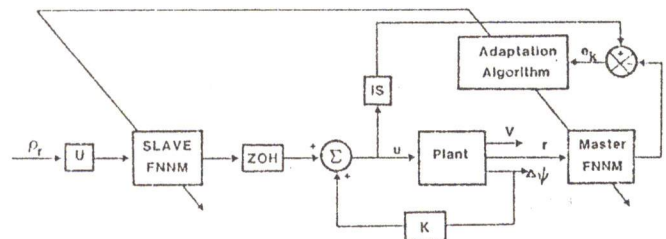$$A = \begin{array}{cc} .07 & .07 \\ .07 & .07 \end{array}$$

Figure 4. Block diagram of FNNM-based control circuit.

The FNN was trained off-line according to the architecture in Figure (5) to minimize the overall error ε^2. Small and random numbers were assigned to the initial weights of the FNN. A plant input was selected and the network was trained to reproduce that input from the plant output. During training stage, a dynamic model of the plant is required.

Since the error signal ($\Delta\psi$) is the feedback signal, training of the network will lead to a gradual switching from feedback to feedforward action as the error signal becomes small.

DISCUSSION OF RESULTS

Computer simulation of the FNN-based controller implemented in the four-wheel-steering system was carried out for a passenger car with the following characteristics: a= 0.946 m, b= 1.719 m, I_{zz}= 2618 Kg.m^2, M_s= 1175 Kg, $C_{\alpha f}$= 48000 N/rad, and $C_{\alpha r}$= 42000 N/rad.
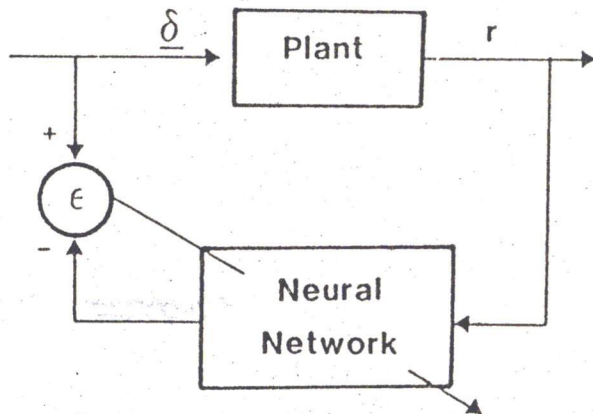

Figure 5. Block learning architecture.

The FNN was trained off-line by repetitively experiencing a selected input pattern to a plant model with U=22.22 m/s (80 km/hr) and W=0. The input pattern was : δ_f =0.024 sin (πS/320) and δ_r=0.0164 sin (πS/320). After learning time of 500 seconds the overall square errors in the front and rear steer angles were minimized to 0.348 *10^{-4} and 0.209*10^{-4}, respectively. Once the FNN learned the inverse dynamic model it was interfaced with the vehicle. The performance of the network was evaluated in the following tasks.

1- Lane-Keeping Task At Different Speeds

The task consists of maintaining the vehicle in the center of the lane while following a curving roadway. The roadway curvature is shown in Figure (6). The system responses were obtained at three vehicle speeds: 27.777 m/s (100 km/hr), 22.22 m/s (80 km/hr), and 16.667 m/s (60 km/hr). Figure (7) shows that no significant discrepancies were detected between the desired and the resulted yaw rate. Although the FNN was trained at U=22.22 m/s, it was able to track the road accurately at faster speed

of 27.77 m/s. The vehicle braking to 16.667 m/s did not affect the system performance. The front and rear-wheel steering angles are illustrated in Figures (8) and (9). No overshoot was exhibited in the response of both angles. For U equal to 16.667 m/s or 22.22 m/s the operation was smooth. As the forward velocity increased to 27.777 m/s, small oscillations were traced, particularly at the end of the road curvature. These oscillations are attributed to the discontinuity at the beginning and the end of the road curvature shown in Figure (6). To eliminate the oscillations, clothoids should be added between road segments. Also, filtering the input to the slave FNN may be justified. This is to account for the fact that drivers often internally generate desired paths which are smoothed version of the commanded path implied by lane centerline. Since the objective of the paper is to investigate the FNN performance for various uncertainties and disturbances, the results were obtained for discontiuous curving roadway. Figures (10) and (11) present the heading and lateral deviations, respectively at different speeds. The heading deviation was kept as small as 0.05 deg. , compared to 0.1 deg. obtained using a preview autopilot control [7], and 0.402 deg. resulted from the driver model [8]. The resulted lateral deviation increased as the vehicle speed increased. The maximum values were 0.01 m, 0.043 m, and 0.094 m for U= 16.667m/s, 22.22 m/s, and 27.777 m/s, respectively.
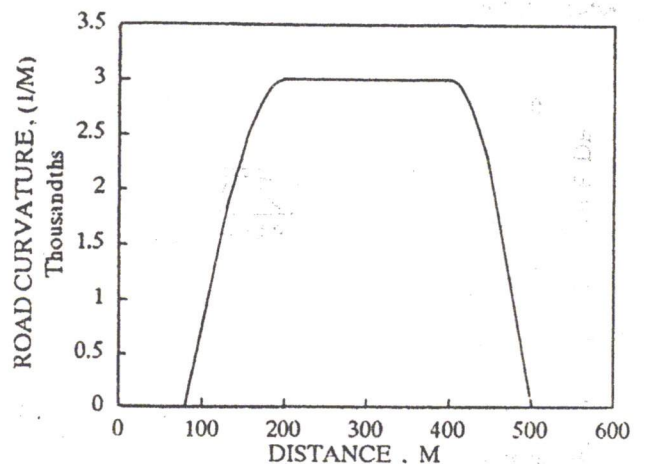

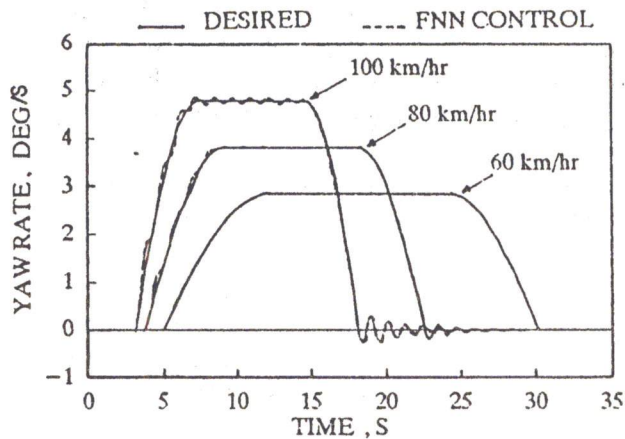Figure 6. Road curvature used in lane-keeping task.

Figure 7. Desired and resulted yaw rate response in lane-keeping task.
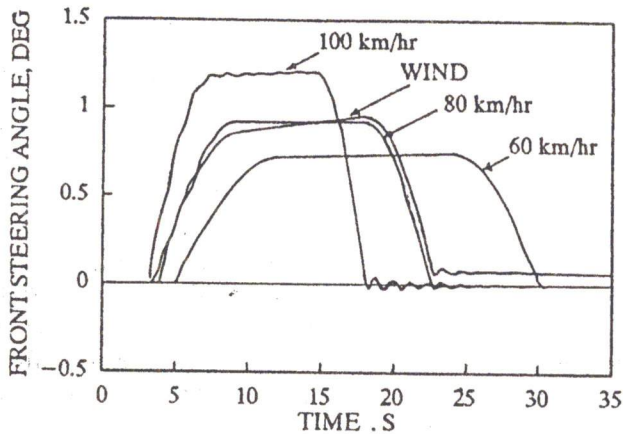

Figure 8. Response of front steering angle in lane-keeping task.
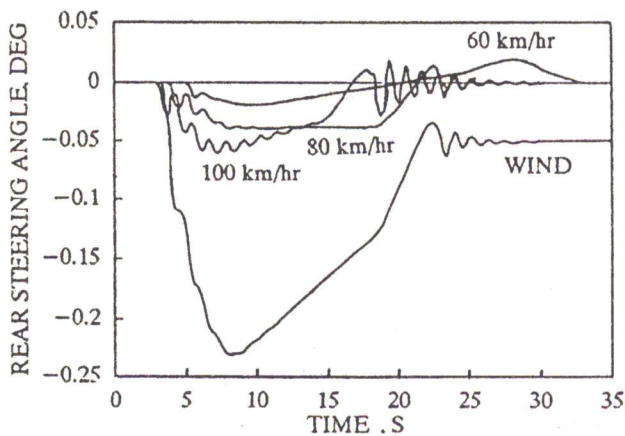

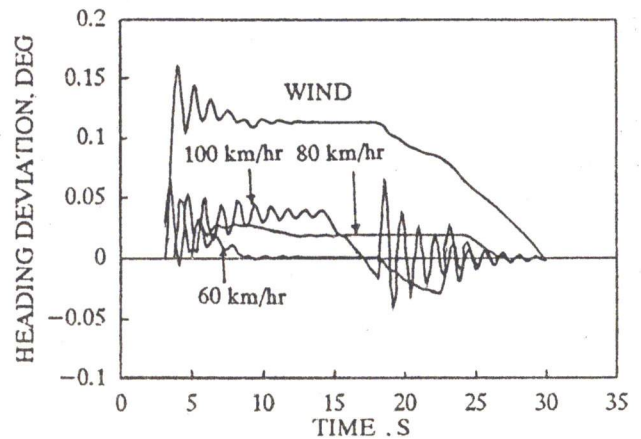Figure 9. Response of rear steering angle in lane-keeping task.

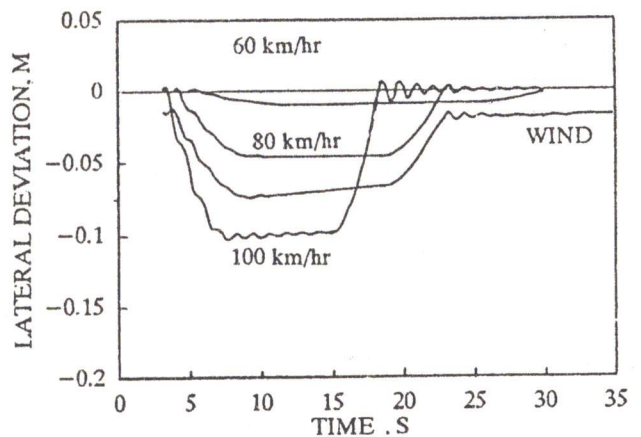Figure 10. Response of heading deviation in lane-keeping task.

Figure 11. Response of lateral deviation in lane-keeping task.

2- Simulation With Side Wind

In this task the car was moving at 22.22 m/s, following the curving roadway shown in Figure (6), and subjected to side wind gusting at a speed of 50 km/hr. As indicated in Equations (1) and (2), the wind produces both torque and lateral force. To overcome the wind effects, the rear wheel steering angle was sharply increased but there was a minimal increase in the front steering angle as shown in Figures (8) and (9). When the car was proceeding along the curved road segment, the control resulted in stable performance with maximum lateral and heading deviations of 0.065m, and 0.1 deg., respectively. As the road became straight, the heading deviation reached its zero value, and the car was laterally displaced by 0.02 m.
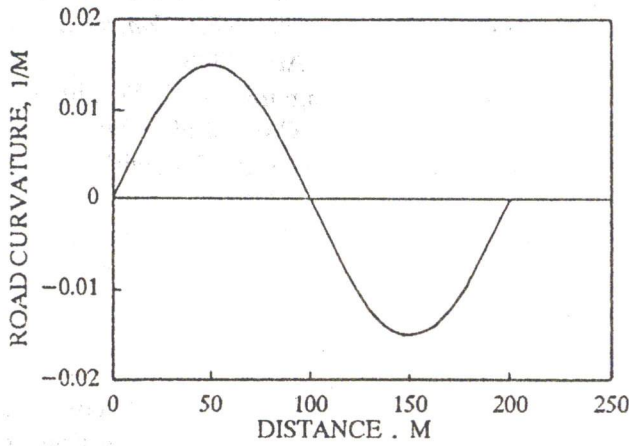
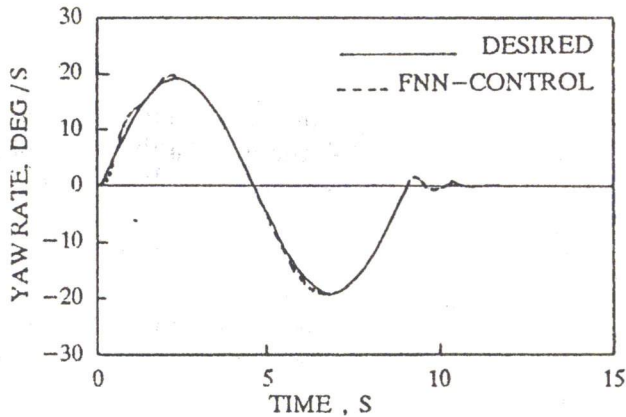Figure 12. Road curvature used in obstacle-avoidance maneuver.

Figure 13. Desired and resulted yaw rate response in obstacle- avoidance maneuver.

3- Obstacle-Avoidance Maneuver

The task involved an aggressive maneuver in which the car had to avoid an obstacle or to pass another car which suddenly appeared in the path. The road curvature for the maneuver is depicted in Figure (12). It was assumed that the car was moving at a speed of 22.22 m/s such that the duration of the maneuver was 9 seconds. The FNNM-based controller displayed a good driving performance during the maneuver. The resulted yaw rate agreed with the desired one as indicated in Figure (13). Due to the sharp changings of the vehicle's heading within short duration, both the maximum heading and lateral deviations (Figures 14, and 15) increased as compared to those associated with task # 1.

Meanwhile, the maximum percentage error in the car heading orientation during sharp maneuver was 0.58% as compared to 0.3% during the gradual heading change.
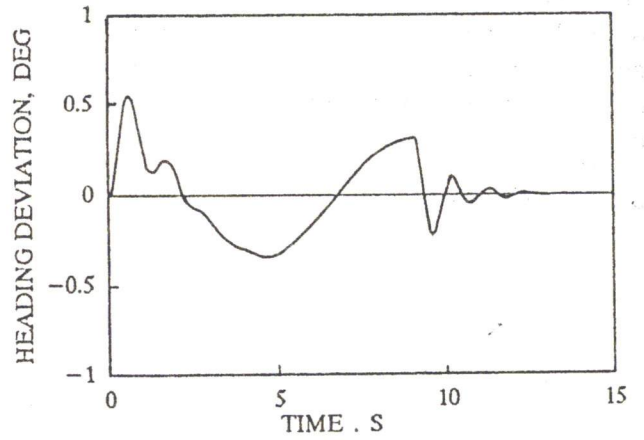

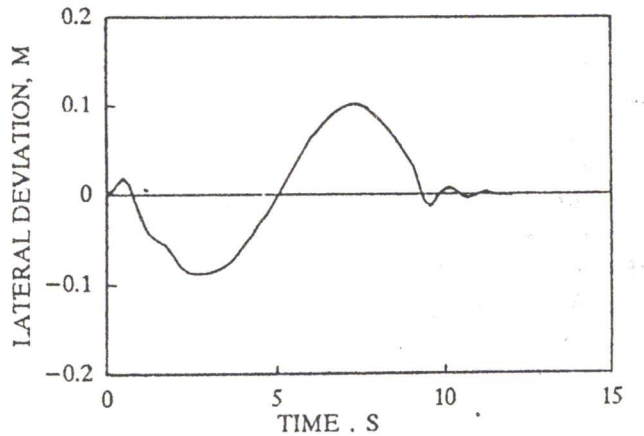Figure 14. Response of heading deviation in obstacle-avoidance maneuver.

Figure 15. Response of lateral deviation in obstacle-avoidance maneuver.

CONCLUSIONS

An automatic feedforward neural network-based control is proposed for FWS passenger cars. Two-layer FNN and generalized adaline weight adaptation algorithm were applied to generate both the front and rear-wheel steer angles. Since the proposed technique requires neither an accurate model nor parameter estimation, a bicycle model of vehicle dynamics was acquired for general training of the network. The learning time duration was 500 s

only. Computer simulation was carried out to evaluate the control system in tasks involving lane keeping on a curving roadway at different speeds, gusting side wind, and an obstacle avoidance maneuver. It was found that the FNN-based control is capable of reproducing the steering behavior of human driver. The system realizes rapid, comfortable, and stable responses in the different tasks.

REFERENCES

[1] S. Sano, and S. Shiraishi, "Four Wheel Steering System With Rear Wheel Steer Angle Controlled as a Function of Steering Wheel Angle", *SAE Paper*, 860625, 1986.

[2] J.C. Whitehead, "Four Wheel Steering: Maneuverability and High Speed Stabilization", *SAE Paper*, 880642, 1988.

[3] A.Y. Lee, "Vehicle Stability Augmentation System Design Using Parameter Optimization", *ASME Journal of Dynamic Systems, Measurement, and Control*, vol. 112, pp 489-495, Sept. 1990.

[4] D. Karnopp and D. Wuh, "Handling Enhancement of Ground Vehicles Using Feedback System Control, *ASME Publications, Advanced Automotive Technologies, DSC*, vol. 13, pp 99-106, 1989.

[5] X. Xia and E.H. Law, "Response of Four-Wheel-Steering Vehicles to Combined Steering and Braking Inputs", *ASME Publications, Advanced Automotive Technologies, DSC*, vol. 13, pp 107-127, 1989.

[6] J. Ackremann and W. Sienel, "Robust Yaw Damping of Cars with Front and Rear Wheel Steering", *IEEE Trans. on Control System Technology*, vol. 1, No. 1, pp 15-20, March 1993.

[7] A.Y. Lee, "A Preview Steering Autopilot Control Algorithm for Four-Wheel-Steering Passenger Vehicles", *ASME Journal of Dynamic Systems, Measurement, and Control*, 1991.

[8] A. Modjtahedzadeh and R.A. Hess, "A Model of Driver Steering Control Behavior for Use in Assesing Vehicle Handling Qualities", *ASME Journal of Dynamic Systems, Measurement, and Control*, vol. 115, pp 456-464, Sept. 1993.

[9] B. Bavarian, "Introduction to Neural Networks for Intelligent Control", *IEEE Control System Mag.*, vol. 8, pp 3-7, Apr. 1988.

[10] T. Shiotsuka, A. Nagamatsu, K. Yoshida and M. Nagaoka, "Active Control of Drive Motion of Four Wheel Steering Car with Neural Network", *SAE Paper*, 940229, 1994.

[11] D. Psaltis, A. Sideris and A.A. Yamamura, "A Multilayered Neural Network Controller", *IEEE Control System Mag.*, vol. 8, pp 17-21, Apr. 1988.

[12] M. Kawato, Y. Uno, M. Isobe and R. Suzuki, "Hierarchial Neural Network Model for Voluntary Movement with Application of Robotics", *IEEE Control System Mag.*, vol. 8, pp. 8-16, Apr. 1988.

[13] D.H. Nguyen and B. Widrow, "Neural Network for Self-Learning Control System", *IEEE Control System Mag.* vol. 10, pp. 18-23, Apr. 1990.

[14] F. Chen, "Back-Propagation Neural Network for Nonlinear Self-Tuning Adaptive Control", *IEEE Control System Mag.*, vol. 10, pp. 44-48, Apr. 1990.

[15] J.G. Kuschewski, S. Hui and S.H. Zak, "Application of Feedforward Neural Networks to Dynamical System Identification and Control", *IEEE Trans. on Control Systems Technology*, vol. 1, No. 1, pp. 37-49, March 1993.

APPENDIX A
Derivation of Equations (1) and(2)

Considering Figure 1, the sum of the yaw moment about the car c.g. yields:

$$a\,F_f\cos\delta_f - b\,F_r\cos\delta_r - LW = I_{zz}\,\dot{r} \quad (A.1)$$

Summing the lateral forces along the body y axis results in:

$$F_f\cos\delta_f + F_r\cos\delta_r - W = M_s\,(\dot{v} + Ur) \quad (A.2)$$

The lateral forces are approximated as:

$$F_f = C_{\alpha f}\,\alpha_f\,,\ F_r = C_{\alpha r}\,\alpha_r \quad (A.3)$$

where $C_{\alpha f}$ and $C_{\alpha r}$ are the cornering stiffness coefficients for the two axles.

For small steering angles, $\cos \delta_f = \cos \delta_r = 1$, and the slip angles are defined as:

$$\alpha_f = \delta_f - (v + ar) / U$$
$$\alpha_r = \delta_r - (v - br) / U \qquad (A.4)$$

Substituting Equations (A.3) and (A.4) into Equations (A.1) and (A.2) results in the following equations of motion:

$$I_{zz}\dot{r} + \frac{(a^2 C_{\alpha f} + b^2 C_{\alpha r})}{U} r + \frac{(aC_{\alpha f} - bC_{\alpha r})}{U} v \qquad (A.5)$$
$$= a\, C_{\alpha f}\delta_f - b\, C_{\alpha r}\delta_r - L\, W$$

$$M_s \dot{v} + (M_s U + \frac{(aC_{\alpha f} - bC_{\alpha r})}{U})r + \frac{C_{\alpha f} + C_{\alpha r}}{U} v \qquad (A.6)$$
$$= C_{\alpha f}\, \delta_f + C_{\alpha r}\, \delta_r - W$$

Equations (A.5) and (A.6) are given in the text as Equations (1) and (2), respectively.